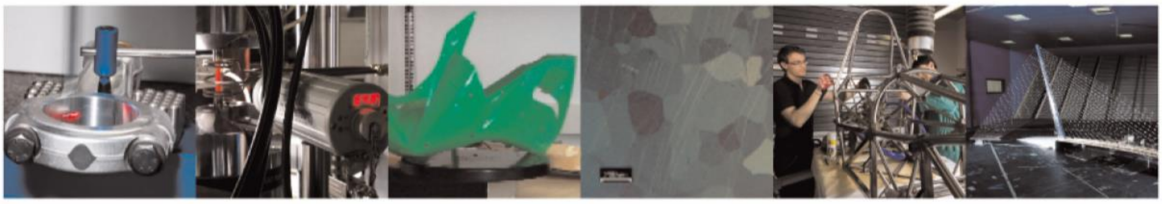

A double shift self-calibration method for micro XY stages

Stefano Petrò

This is a post-peer-review, pre-copyedit version of an article published in Precision Engineering. The final authenticated version is available online at:
http://dx.doi.org/10.1016/j.precisioneng.2019.02.005

DIPARTIMENTO DI MECCANICA ■ POLITECNICO DI MILANO
via G. La Masa, 1 ■ 20156 Milano ■ EMAIL (PEC): pecmecc@cert.polimi.it
http://www.mecc.polimi.it
Rev. 0

A double shift self-calibration method for micro XY stages

Stefano Petrò[a,*]

[a] *Department of Mechanical Engineering, Politecnico di Milano, Via La Masa 1, 20156, Milano, Italy*

Abstract

In most cases calibration of measuring instruments is obtained by comparing measurement results to a measurement standard. But in the case of coordinate measuring system, the availability of reliable measurement standards is often limited: calibrated ball plated, for example, are expensive and difficult to maintain. This originated the so called "self-calibration" procedures, in which an uncalibrated artifact is adopted to estimate the stage error of the system.

One of the most widespread coordinate measuring systems is an XY stage. Several procedures have been proposed for the self-calibration of this kind of system. Most of them are based on performing three or more measurements of an uncalibrated plate, with the position of the plate changing from one measurement to the other. Oftentimes, the positions are only slightly different from each other, thus making it difficult to obtain them with a good accuracy when measurements are carried out at a micro scale. In this work, an approach is proposed which allows larger displacement from one measurement to the others, thereby allowing an easier management for micro XY stages.

Keywords:
XY stage; self-calibration; stage error compensation; uncalibrated artifact.

1. Calibration and self-calibration

Calibration is the key to the accuracy of any measuring instrument. According to the International Vocaboulary of Metrology (VIM) [1], the calibration is defined as

> operation that, under specified conditions, in a first step, establishes a relation between the quantity values with measurement uncertainties provided by measurement standards and corresponding

*Correspondig Author. Tel +39 02 23998530. Fax +39 02 23998585.
Email address: `stefano.petro@polimi.it` (Stefano Petrò)

indications with associated measurement uncertainties and, in a second step, uses this information to establish a relation for obtaining a measurement result from an indication.

According to this definition, without calibration it is impossible to state that measurements are traceable to the reference measurement unit, whereupon measurement trueness is impossible to guarantee. But most often, calibration is not only intended as the operation which "creates the link" between a measurement standard and the measurement result, and is also intended as the operation which guarantees the measuring system behaves to its best capability. In practical terms, it identifies the systematic measurement errors, allowing their correction. According to the VIM, this operation should be called "adjustment of a measuring system", but is commonly referred to as "calibration".

Like any other measuring instrument, coordinate measuring systems (CMSs), too, need calibration. As most CMSs consist in a series of axes working together to provide a measurement result, the traditional measurement standard adopted as reference to calibrate them is a laser interferometer: each axis is tested against it singularly. Although some different approaches have been proposed [2], in general testing the axes separately is not considered sufficient, because they often interact. The choice artifacts made up of a series of regular "sub-artifacts" (marks, hole, hemispheres, spheres, etc.) regularly distributed on a plate as calibrated measurement standards are then quite common where high accuracy is required. However, calibrated plates are expensive and difficult to maintain.

To overcome this limitation, "self-calibration" [3, 4] techniques have been introduced. In self-calibration techniques, an uncalibrated artifact is used instead of a calibrated measurement standard. As such, a direct identification of measurement errors is impossible. Therefore, repeated measurements in varying conditions are conducted. In the absence of random measurement errors, the analysis of the measurement results leads to both the identification of the systematic volumetric measurement errors (usually in limited sets of locations) and the calibration of the artifact (with the identification of the deviation from the nominal geometry) - the so called "separation". Most often, the adopted reference artifact is a plate with sub-artifacts. Many self-calibration approaches have been proposed in the past for CMSs [5, 6].

Among the others, a method for the self-calibration of XY stages has been proposed by Ye *et al.* [7] that involves the measurement of a square plate, which brings a series of sub-artifact on an evenly spaced on grid; the distance between two sub-artifacts is Δ, and there are N sub-artifacts along each side of the artifact. The aim is to evaluate the systematic component of the volumetric measurement error as a function of the probing location, but only in those locations which correspond to a sub-artifact. Reference (Cartesian) axes can be defined for both the artifact and the measuring device. To obtain an evaluation the stage error at the artifact locations, according to Ye *et al.*, the plate has to be measured in three positions (views):

- **View 0**. This is the original view - the reference system of the plate nominally corresponds to the reference system of the measuring system.

- **View 1**. The plate is 90° counterclockwise rotated, in respect of the measuring device reference system.
- **View 2**. The artifact is translated by Δ, in the positive x direction, with respect to the measuring device reference system.

The proposed result is an analytical solution, which, in the absence of random measurement errors, decompose the measurement results into the plate deviations from the nominal geometry and the systematic stage errors. Several evolutions and inspired approaches have been proposed [8, 9, 10, 11, 12, 13, 14, 15, 16, 17], including approaches dealing with coordinate measuring machines [9, 13], rotary stages [14], and $XY\theta_z$ stages [11].

This work is a further derivation of the Ye *et al.* method. It has been designed for the case in which micro-stages XY must be calibrated. In this case very small plates [18] are required. For such small plates, the Δ displacement is usually obtained by grooving on the plate side opposite to the sub-artifacts two series of V-groves spaced by 120°, which can be coupled with three spheres constituting a kinematic mount. But if Δ is small (1 mm or even less), the grooves will be very close to each other and then very small themselves, making their accurate manufacture difficult or even impossible. A methodology allowing a displacement larger than Δ is available, this could make the manufacture of accurate small plates easier. The proposed method allows for larger displacement of the plate. Actually, a modification of the mathematics of Ye *et al.* method allow a shift equal to twice the distance between the sub-artifacts of the plate. This requires the addition of a "view 3" in which the plate is shifted by 3Δ in the opposite direction of view 2, but with only a limited number of measurements performed in it. Furthermore, this paper states that a further increase of the displacement is impossible without a complete modification of the approach. To show the theoretical performance of the method, it is validated by means of simulation.

2. Procedure for the double-step self-calibration

As stated previously, when the sub-artifacts are very close to each other, i.e. when Δ is very small, obtaining the 1Δ translation required by Ye *et al.* method can be very difficult. One could then wonder whether the mathematics of the method allow for a larger displacement. In the following, it will be demonstrated that it is possible to have self-calibration and separation if a view with a 2Δ translation in the positive direction is taken together with an additional view with a 3Δ translation in the negative direction. The proposed method will be defined as "double step" self-calibration.

The four views required by the method are then as follows (Fig. 1):

- **View 0**. This is the original view - the reference system of the plate nominally corresponds to the reference system of the measuring system.

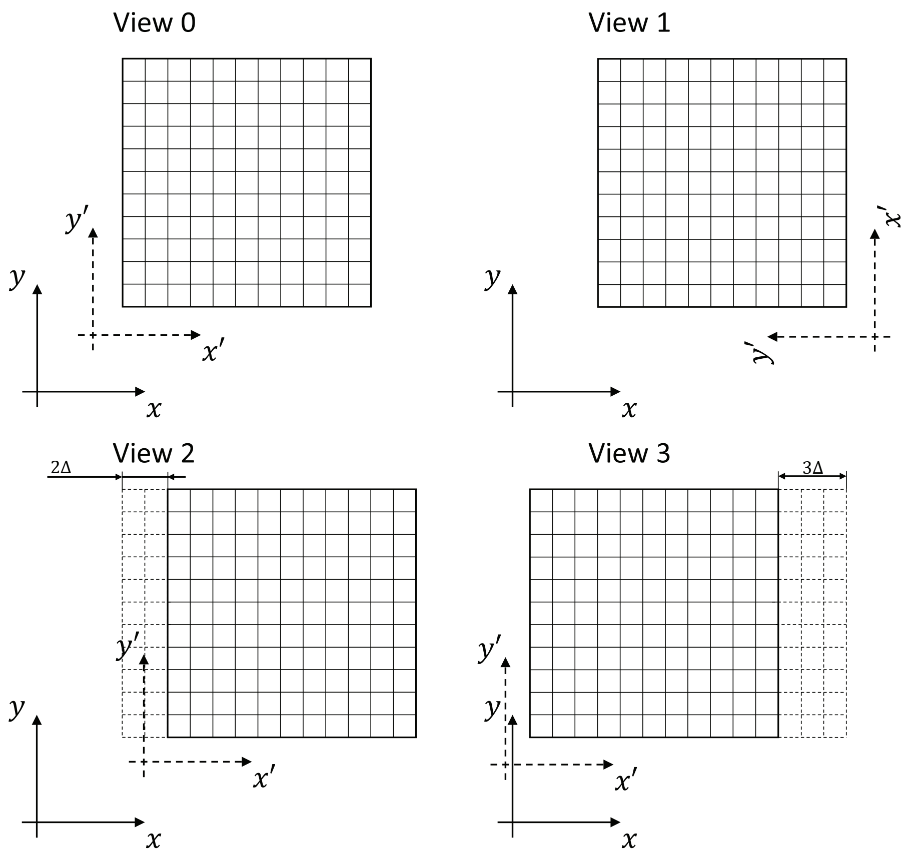

Figure 1: Views required by the "double step" method. xy denotes the XY stage reference system, $x'y'$ denotes the plate reference system.

- **View 1**. In this view the plate is 90° counterclockwise rotated, in respect of the measuring device reference system.
- **View 2**. In view two the artifact is translated by 2Δ, in the *positive* x direction, in respect of the measuring device reference system.
- **View 3**. In view three the artifact is translated by 3Δ, in the *negative* x direction, in respect of the measuring device reference system. In this view, it is not required to sample the whole plate. It suffices to sample the central row of the array, and two adjacent columns (in the following, it will be supposed that the central column and its adjacent column on the positive x direction are sampled).

The plate adopted must have an odd and identical number of rows and columns N, and $N \geq 9$. It is worth noting that actually only a row and a column measurement must be added, compared to the Ye *et al.* method.

3. Mathematical model

Ye *et al.* originally proposed their model in an algebraic formulation. However, the data structure (coordinates of points belonging to an evenly spaced grid) suggests that a matrix formulation is possible.This matrix formulation is easier to understand, too, so the methodology will be proposed in such form. A Mathworks Matlab© script is attached to illustrate a practical example of application [19].

Before describing the methodology, let us define few scalars, vectors and matrices which will be of assistance for a better comprehension.

- $s = (N-1)/2 + 1$.
- $\mathbf{1}_k = [x_{i,1}], x_{i,1} = 1 \forall i \in \{1, \ldots, k\}$

  $\mathbf{1}_k$ is simply a column vector made up only by "1". For notation simplicity, $\mathbf{1}_N = \mathbf{1}$.
- $\mathbf{E}_k = [x_{i,j}], i \in \{1, \ldots, N\}, j \in \{1, \ldots, N-k\}, x_{i,j} = \begin{cases} 1, & i = j \\ 0, & i \neq j \end{cases}$

  $\mathbf{ME}_k$ is a matrix identical to $\mathbf{M}$ deprived of the last k columns. For notation simplicity, $\mathbf{E} = \mathbf{E}_2$.
- $\mathbf{S} = [x_{i,j}], i, j \in \{1, \ldots, N\}, x_{i,j} = \begin{cases} 1, & i = N - j + 1 \\ 0, & i \neq N - j + 1 \end{cases}$

  Post-multiplying matrix $\mathbf{M}$ time $\mathbf{S}$ has the effect of swapping the first column with the last, the second with the penultimate, and so on, and similarly pre-multiplying swaps rows. Please note that $\mathbf{S}$ is a symmetric and orthogonal matrix.
- $\mathbf{T}_k = [x_{i,j}], i, j \in \{1, \ldots, N\}, x_{i,j} = \begin{cases} 1, & i = j + k \\ 1, & i = j + k - N \\ 0, & \text{else} \end{cases}$

  Post-multiplying matrix $\mathbf{M}$ time $\mathbf{T}_k$ has the effect of "rotating" the columns of $\mathbf{M}$, that is, the $k^{\text{th}}+1$ column of $\mathbf{M}$ becomes the first, the $(k+2)^{\text{th}}$ column becomes the second, etc., while the first column becomes the $N-k+1$ column and so on. Please note that $\mathbf{T}_k$ is an orthogonal matrix.
- $\mathbf{O}_{\mathbf{T}} = [x_{i,j}], i, j \in \{1, \ldots, N\}, x_{i,j} = \begin{cases} 1, & i > j \wedge i + j \quad \text{is even} \\ 0, & \text{else} \end{cases}$
- $\mathbf{X} = [x_{i,j}], i, j \in \{1, \ldots, N\}, x_{i,j} = \Delta (j - s)$

  $\mathbf{Y} = [x_{i,j}], i, j \in \{1, \ldots, N\}, x_{i,j} = \Delta (i - s)$

  $\mathbf{X}$ and $\mathbf{Y}$ are auxiliary matrices which contain the nominal coordinates of the points in the grid. Please note that $\mathbf{X} = \mathbf{Y}^{\mathrm{T}}$, where $^{\mathrm{T}}$ denotes the matrix transposition.

3.1. Assumptions on the stage error model

Exactly the same assumptions taken by Ye *et al.* are taken here. The stage error at location (x, y) can be defined by a two dimensional function $\mathbf{G}(x, y) = G_x(x, y)\,\mathbf{e}_x + G_y(x, y)\,\mathbf{e}_y$, where $\mathbf{e}_x, \mathbf{e}_y$ are the x and y direction vectors of the stage and $G_x(x, y), G_y(x, y)$ are 2-dimensional functions defined at any position the moving stage can reach. The goal of self-calibration is the definition of this function, at least on a discrete number of locations. If we consider only a NxN set of locations, the $G_x(x, y), G_y(x, y)$ functions can be represented by a couple of NxN matrices $\mathbf{G}_x, \mathbf{G}_y$, in which the (n, m) element defines the stage error at the coordinates $x = (m - s)\,\Delta, \quad y = (n - s)\,\Delta$ in the measuring device reference system.

The stage error is assumed to have the following properties:

- *No translation.*

$$\begin{aligned} \mathbf{1}^{\mathrm{T}}\mathbf{G}_x\mathbf{1} &= 0 \\ \mathbf{1}^{\mathrm{T}}\mathbf{G}_y\mathbf{1} &= 0 \end{aligned} \tag{1}$$

- *No rotation.*

$$\mathbf{1}^{\mathrm{T}}\left(\mathbf{X}\mathbf{G}_y^{\mathrm{T}} - \mathbf{Y}^{\mathrm{T}}\mathbf{G}_x\right)\mathbf{1} = 0 \tag{2}$$

  Translation and rotation of matrices $\mathbf{G}_x$ and $\mathbf{G}_y$ depends only on the choice of measuring device reference system, and are therefore not relevant in the definition of the stage error.

- *No magnification.*

$$\mathbf{1}^{\mathrm{T}}\left(\mathbf{X}\mathbf{G}_x^{\mathrm{T}} + \mathbf{Y}^{\mathrm{T}}\mathbf{G}_y\right)\mathbf{1} = 0 \tag{3}$$

  The absence of magnification in $\mathbf{G}_x, \mathbf{G}_y$ is hard to justify. In fact, it implies *de facto* that the measuring system is metrologically traceable. This in general requires calibration of the system, and as such is in contrast with the idea of applying self-calibration. As such, to at least reduce the impact of this assumption, it is suggested that the axes of the XY stage (considered separately) are calibrated.

Two *first order* stage errors can now be introduced:

- *Non orthogonality error.* The non-orthogonality error is due to the fact that the axes of the measuring device are not perfectly perpendicular. The non-orthogonality error can be measured by the O index:

$$O = \frac{\mathbf{1}^{\mathrm{T}}\left(\mathbf{X}\mathbf{G}_y^{\mathrm{T}} + \mathbf{Y}^{\mathrm{T}}\mathbf{G}_x\right)\mathbf{1}}{\mathbf{1}^{\mathrm{T}}\left(\mathbf{X}\mathbf{X}^{\mathrm{T}} + \mathbf{Y}^{\mathrm{T}}\mathbf{Y}\right)\mathbf{1}} \tag{4}$$

- *Scale error.* Scale error measures the different linearity of the axes, and can be measured by the R index:

$$R = \frac{\mathbf{1}^{\mathrm{T}}\left(\mathbf{X}\mathbf{G}_x^{\mathrm{T}} - \mathbf{Y}^{\mathrm{T}}\mathbf{G}_y\right)\mathbf{1}}{\mathbf{1}^{\mathrm{T}}\left(\mathbf{X}\mathbf{X}^{\mathrm{T}} + \mathbf{Y}^{\mathrm{T}}\mathbf{Y}\right)\mathbf{1}} \tag{5}$$

Finally, any other stage error is taken into account by the *second order* stage errors $\mathbf{F}_x, \mathbf{F}_y$, so that

$$\begin{aligned} \mathbf{G}_x &= O\mathbf{Y} + R\mathbf{X} + \mathbf{F}_x \\ \mathbf{G}_y &= O\mathbf{X} - R\mathbf{Y} + \mathbf{F}_y \end{aligned} \tag{6}$$

The second order errors retains the $\mathbf{G}$ properties defined in (1), (2), and (3),and has also the *no non orthogonality* and *no scale error* properties. The properties of the second order errors can be summarized as:

$$\begin{aligned} \mathbf{1}^{\mathrm{T}}\mathbf{X}\mathbf{F}_x^{\mathrm{T}}\mathbf{1} = \mathbf{1}^{\mathrm{T}}\mathbf{Y}^{\mathrm{T}}\mathbf{F}_x\mathbf{1} = \mathbf{1}^{\mathrm{T}}\mathbf{F}_x\mathbf{1} \quad &= 0 \\ \mathbf{1}^{\mathrm{T}}\mathbf{X}\mathbf{F}_y^{\mathrm{T}}\mathbf{1} = \mathbf{1}^{\mathrm{T}}\mathbf{Y}^{\mathrm{T}}\mathbf{F}_y\mathbf{1} = \mathbf{1}^{\mathrm{T}}\mathbf{F}_y\mathbf{1} \quad &= 0 \end{aligned} \tag{7}$$

3.2. Assumptions on the artifact model

The deviation from the nominal coordinates for the set of sub-artifact at location (x, y) can be defined by a couple of NxN matrices $\mathbf{A}_x, \mathbf{A}_y$, in which the (n, m) element defines the deviation at the coordinates $x = (m - s)\,\Delta, \quad y = (n - s)\,\Delta$ in the artifact reference system.

Like the stage error, artifact error is endowed with some properties:

- *No translation.*

$$\begin{aligned} \mathbf{1}^{\mathrm{T}}\mathbf{A}_x\mathbf{1} &= 0 \\ \mathbf{1}^{\mathrm{T}}\mathbf{A}_y\mathbf{1} &= 0 \end{aligned} \tag{8}$$

- *No rotation.*

$$\mathbf{1}^{\mathrm{T}}\left(\mathbf{X}\mathbf{A}_y^{\mathrm{T}} - \mathbf{Y}^{\mathrm{T}}\mathbf{A}_x\right)\mathbf{1} = 0 \tag{9}$$

Again, these properties are essentially due to the arbitrariness of the plate reference system.

4. Measurement and measurement results analysis

Views 0 and 1 for the present methodology are identical to those proposed by Ye *et al.*. As such, only the relevant results for view 0 and 1 are reported here. For further information, please refer to Ye *et al.* works.

The following discussion does not consider the random measurement error. If the random measurement error is not present, then the methodology is able to exactly reconstruct the stage error. The impact of the random error will be discussed later.

4.1. View 0

In view zero, the measuring device reference system and the artifact reference system are nominally coincident. Of course, some positioning error is unavoidable, which leads to the translational misalignment t_{0x}, t_{0y} in the x and y direction of the measuring device reference system respectively, and the rotational misalignment θ_0. The measurement result can be expressed by the matrices $\mathbf{V}_{0,x}, \mathbf{V}_{0,y}$, in which the (n, m) element defines the measured deviation (in the measuring device reference system) from the nominal position for the sub-artifact located at $x = (m - s)\,\Delta, \quad y = (n - s)\,\Delta$ in the artifact reference system. Mathematically, if no random error is present, and θ_0 is small, the measurement result may be expressed as follows:

$$\begin{aligned} \mathbf{V}_{0,x} &= \mathbf{G}_x + \mathbf{A}_x - \theta_0 \mathbf{Y} + \mathbf{1}\mathbf{1}^{\mathrm{T}} t_{0x} \\ \mathbf{V}_{0,y} &= \mathbf{G}_y + \mathbf{A}_y + \theta_0 \mathbf{X} + \mathbf{1}\mathbf{1}^{\mathrm{T}} t_{0y} \end{aligned} \tag{10}$$

Based on this formulation, and on the properties of $\mathbf{G}_x, \mathbf{G}_y, \mathbf{A}_x, \mathbf{A}_y$, it is possible to evaluate the misalignment parameters (please note that $\mathbf{1}^{\mathrm{T}}\mathbf{X}\mathbf{1} = \mathbf{1}^{\mathrm{T}}\mathbf{Y}\mathbf{1} = 0$):

$$\begin{aligned} t_{x0} &= \mathbf{1}^{\mathrm{T}} \mathbf{V}_{0,x} \mathbf{1} / N^2 \\ t_{y0} &= \mathbf{1}^{\mathrm{T}} \mathbf{V}_{0,y} \mathbf{1} / N^2 \end{aligned} \tag{11}$$

$$\theta_0 = \frac{\mathbf{1}^{\mathrm{T}} \left(\mathbf{X}\mathbf{V}_{0,y}^{\mathrm{T}} - \mathbf{Y}^{\mathrm{T}} \mathbf{V}_{0,x} \right) \mathbf{1}}{\mathbf{1}^{\mathrm{T}} \left(\mathbf{Y}^{\mathrm{T}}\mathbf{Y} + \mathbf{X}\mathbf{X}^{\mathrm{T}} \right) \mathbf{1}} \tag{12}$$

4.2. View 1

In view 1 the artifact is 90° counterclockwise rotated in respect of the measuring device reference system. Again, misalignment can be expressed by the terms t_{1x}, t_{1y}, and θ_1. The measurement result can be expressed by the matrices $\mathbf{V}_{1,x}, \mathbf{V}_{1,y}$. The measurement results expression is the following:

$$\begin{aligned} \mathbf{V}_{1,x} &= \mathbf{S}\mathbf{G}_x^{\mathrm{T}} - \mathbf{A}_y - \theta_1 \mathbf{X} + \mathbf{1}\mathbf{1}^{\mathrm{T}} t_{1x} \\ \mathbf{V}_{1,y} &= \mathbf{S}\mathbf{G}_y^{\mathrm{T}} + \mathbf{A}_x - \theta_1 \mathbf{Y} + \mathbf{1}\mathbf{1}^{\mathrm{T}} t_{1y} \end{aligned} \tag{13}$$

Again, it is possible to evaluate the misalignment parameters:

$$\begin{aligned} t_{x1} &= \mathbf{1}^{\mathrm{T}} \mathbf{V}_{1,x} \mathbf{1} / N^2 \\ t_{y1} &= \mathbf{1}^{\mathrm{T}} \mathbf{V}_{1,y} \mathbf{1} / N^2 \end{aligned} \tag{14}$$

$$\theta_1 = \frac{\mathbf{1}^{\mathrm{T}} \left(-\mathbf{X}\mathbf{V}_{1,x}^{\mathrm{T}} - \mathbf{Y}^{\mathrm{T}} \mathbf{V}_{1,y} \right) \mathbf{1}}{\mathbf{1}^{\mathrm{T}} \left(\mathbf{X}\mathbf{X}^{\mathrm{T}} + \mathbf{Y}^{\mathrm{T}}\mathbf{Y} \right) \mathbf{1}} \tag{15}$$

4.2.1. Evaluation of the first order error terms

Based on the measurement results in view 0 and view 1, it is possible to evaluate the first order error terms. First of all, let us remove the misalignment from the measurement results, defining the $\mathbf{U}$ matrices:

$$\begin{aligned}\mathbf{U}_{0,x} = \quad & \mathbf{V}_{0,x} + \theta_0\mathbf{Y} - \mathbf{1}\mathbf{1}^{\mathrm{T}}t_{0x} = \quad & \mathbf{G}_x + \mathbf{A}_x = \quad & O\mathbf{Y} + R\mathbf{X} + \mathbf{F}_x + \mathbf{A}_x \\ \mathbf{U}_{0,y} = \quad & \mathbf{V}_{0,y} - \theta_0\mathbf{X} - \mathbf{1}\mathbf{1}^{\mathrm{T}}t_{0y} = \quad & \mathbf{G}_y + \mathbf{A}_y = \quad & O\mathbf{X} - R\mathbf{Y} + \mathbf{F}_y + \mathbf{A}_y\end{aligned} \tag{16}$$

$$\begin{aligned}\mathbf{U}_{1,x} = \quad & \mathbf{V}_{1,x} + \theta_1\mathbf{X} - \mathbf{1}\mathbf{1}^{\mathrm{T}}t_{1x} = \quad & O\mathbf{Y}^{\mathrm{T}} - R\mathbf{X}^{\mathrm{T}} + \mathbf{S}\mathbf{F}_x^{\mathrm{T}} - \mathbf{A}_y \\ \mathbf{U}_{1,y} = \quad & \mathbf{V}_{1,y} + \theta_1\mathbf{Y} - \mathbf{1}\mathbf{1}^{\mathrm{T}}t_{1y} = \quad & -O\mathbf{X}^{\mathrm{T}} - R\mathbf{Y}^{\mathrm{T}} + \mathbf{S}\mathbf{F}_y^{\mathrm{T}} + \mathbf{A}_x\end{aligned} \tag{17}$$

by summing or subtracting (16) and (17) the following system of equations, which gets rid of the artifact error $\mathbf{A}_x, \mathbf{A}_y$, we can obtain:

$$\begin{cases}\mathbf{U}_{0,x} - \mathbf{U}_{1,y} = 2O\mathbf{Y} + 2R\mathbf{X} + \mathbf{F}_x - \mathbf{S}\mathbf{F}_y^{\mathrm{T}} \\ \mathbf{U}_{0,y} + \mathbf{U}_{1,x} = 2O\mathbf{X} - 2R\mathbf{Y} + \mathbf{F}_y - \mathbf{S}\mathbf{F}_x^{\mathrm{T}}\end{cases} \tag{18}$$

Solving (18) for O and R, remembering properties (7), yields (19) and (20), which allows the evaluation of O and R respectively:

$$O = \frac{\mathbf{1}^{\mathrm{T}}\left(\mathbf{X}\mathbf{U}_{0,x} - \mathbf{X}\mathbf{U}_{1,y} + \mathbf{Y}^{\mathrm{T}}\mathbf{U}_{0,y}^{\mathrm{T}} + \mathbf{Y}^{\mathrm{T}}\mathbf{U}_{1,x}^{\mathrm{T}}\right)\mathbf{1}}{2\cdot\mathbf{1}^{\mathrm{T}}\left(\mathbf{X}\mathbf{X}^{\mathrm{T}} + \mathbf{Y}^{\mathrm{T}}\mathbf{Y}\right)\mathbf{1}} \tag{19}$$

$$R = \frac{\mathbf{1}^{\mathrm{T}}\left(\mathbf{Y}^{\mathrm{T}}\mathbf{U}_{0,x}^{\mathrm{T}} - \mathbf{Y}^{\mathrm{T}}\mathbf{U}_{1,y}^{\mathrm{T}} - \mathbf{X}\mathbf{U}_{0,y} - \mathbf{X}\mathbf{U}_{1,x}\right)\mathbf{1}}{2\cdot\mathbf{1}^{\mathrm{T}}\left(\mathbf{X}\mathbf{X}^{\mathrm{T}} + \mathbf{Y}^{\mathrm{T}}\mathbf{Y}\right)\mathbf{1}} \tag{20}$$

4.2.2. Evaluation of the real part of the Fourier transform of $\mathbf{F}_x$ and $\mathbf{F}_y$

View 0 and view 1 are not sufficient to completely define the error map $\mathbf{G}_x, \mathbf{G}_y$. In fact, they are the same view rotated by 90°, and therefore they cannot point out any rotational symmetric error: at least a translational view is required. However, most of the stage errors may be derived from these two views.

In the following, an approach based on the Fourier transforms will be proposed. Of course, knowledge of the 2D Discrete Fourier Transform (DFT) of $\mathbf{F}_x$ and $\mathbf{F}_y$, plus the already calculated O and R indexes is equivalent to the complete knowledge of $\mathbf{G}_x$ and $\mathbf{G}_y$.

First of all, we get rid of scale error and non-orthogonality error by defining the following matrices:

$$\begin{aligned}\mathbf{P} = & \mathbf{U}_{0,x} - \mathbf{U}_{1,y} - 2O\mathbf{Y} - 2R\mathbf{X} \quad & = \mathbf{F}_x - \mathbf{S}\mathbf{F}_y^{\mathrm{T}} \\ \mathbf{Q} = & \mathbf{U}_{0,y} + \mathbf{U}_{1,x} - 2O\mathbf{X} + 2R\mathbf{Y} \quad & = \mathbf{F}_y + \mathbf{S}\mathbf{F}_x^{\mathrm{T}}\end{aligned} \tag{21}$$

The following result may be obtained:

$$\mathbf{P} + \mathbf{S}\mathbf{Q}^{\mathrm{T}} - \mathbf{S}\mathbf{P}\mathbf{S} - \mathbf{Q}^{\mathrm{T}}\mathbf{S} = \mathbf{0} \tag{22}$$

which implies that there is a linear dependence between $\mathbf{P}$ and $\mathbf{Q}$. Therefore, (21) is not sufficient to completely describe $\mathbf{F}_x$ and $\mathbf{F}_y$ - the rotational symmetric terms of the stage error cannot be identified by view 0 and view 1 only.

2D DFT can be computed, in matrix form, by pre- and post-multiplying time a special matrix $\mathbf{W}$. In this work, we are not considering the classical DFT matrix [20]. The formulation considered here is the following:

$$\mathbf{W} = [x_{h,k}]\,, h, k \in \{1, \ldots, N\}\,, x_{h,k} = \frac{1}{N} e^{\frac{-2\pi i(h-1-(N-1)/2)(k-1-(N-1)/2)}{N}} \tag{23}$$

It is possible to shift from classical DFT and DFT obtained with this matrix by simply reordering rows and columns, and by applying the shift theorem [20]. However, $\mathbf{W}$ matrix and transforms obtained by it have some properties (provided they are applied to a real matrix $\mathbf{M}$) which will ease the self-calibration methodology demonstration:

$$\begin{aligned} \mathbf{W} &= \mathbf{W}^{\mathrm{T}} \\ \mathbf{SW} &= \mathbf{WS} \\ N\mathbf{WSW} &= \mathbf{I} \\ \mathbf{SWMW} &= (\mathbf{WMWS})^{*} \\ \mathbf{WM}^{\mathrm{T}}\mathbf{W} &= (\mathbf{WMW})^{\mathrm{T}} \end{aligned} \tag{24}$$

where * denotes complex conjugate. After some manipulation, it is possible to apply DFT to $\mathbf{P}$ and $\mathbf{Q}$:

$$\begin{aligned} \mathbf{WPW} &= \mathbf{WF}_x\mathbf{W} - \mathbf{WSF}_y^{\mathrm{T}}\mathbf{W} \\ \mathbf{WQ}^{\mathrm{T}}\mathbf{SW} &= \mathbf{WF}_y^{\mathrm{T}}\mathbf{SW} + \mathbf{WF}_x\mathbf{W} \end{aligned} \tag{25}$$

Applying the properties in (24), from (25) we obtain the following (26):

$$\begin{aligned} \mathbf{WPW} &= \mathbf{WF}_x\mathbf{W} - \mathbf{SWF}_y^{\mathrm{T}}\mathbf{W} \\ \mathbf{WQ}^{\mathrm{T}}\mathbf{SW} &= \left(\mathbf{SWF}_y^{\mathrm{T}}\mathbf{W}\right)^{*} + \mathbf{WF}_x\mathbf{W} \end{aligned} \tag{26}$$

From this result it is possible to obtain the real part of the transform of $\mathbf{F}_x$ and $\mathbf{F}_y$:

$$\begin{aligned} \operatorname{Re}(\mathbf{WF}_x\mathbf{W}) &= \frac{1}{2}\operatorname{Re}\left(\mathbf{WPW} + (\mathbf{WQW})^{\mathrm{T}}\mathbf{S}\right) \\ \operatorname{Re}\left(\mathbf{S}(\mathbf{WF}_y\mathbf{W})^{\mathrm{T}}\right) &= \frac{1}{2}\operatorname{Re}\left((\mathbf{WQW})^{\mathrm{T}}\mathbf{S} - \mathbf{WPW}\right) \end{aligned} \tag{27}$$

Unfortunately, it is not sufficient to obtain the imaginary part of the transform. However, it is sufficient to obtain the following linear relationship:

$$\operatorname{Im}\left(\mathbf{WF}_x\mathbf{W} - \mathbf{S}(\mathbf{WF}_y\mathbf{W})^{\mathrm{T}}\right) = \frac{1}{2}\operatorname{Im}\left(\mathbf{WPW} + (\mathbf{WQW})^{\mathrm{T}}\mathbf{S}\right) \tag{28}$$

4.3. View 2

In view 2 the artifact is shifted by an amount 2Δ in the positive x direction of the measuring device reference system. As in view 0 and 1, misalignment can be expressed by the terms t_{2x}, t_{2y}, and θ_2. The measurement result can be expressed by the matrices $\mathbf{V}_{2,x}, \mathbf{V}_{2,y}$. It is possible to express mathematically the measurement results by means of multiplication of the various matrices expressing artifact and stage error time $\mathbf{T}_2$. The measurement results expression is the following:

$$\begin{aligned}
\mathbf{V}_{2,x}\mathbf{E} &= \left(\mathbf{G}_x\mathbf{T}_2 + \mathbf{A}_x - \theta_2\mathbf{Y} + \mathbf{1}\mathbf{1}^{\mathrm{T}}t_{2x}\right)\mathbf{E} \\
\mathbf{V}_{2,y}\mathbf{E} &= \left(\mathbf{G}_y\mathbf{T}_2 + \mathbf{A}_y + \theta_2\mathbf{X} + \mathbf{1}\mathbf{1}^{\mathrm{T}}t_{2y}\right)\mathbf{E}
\end{aligned} \tag{29}$$

Please note that the last two columns of $\mathbf{V}_{2,x}$ and $\mathbf{V}_{2,y}$ do not actually exist: in fact, the artifact columns of sub-artifacts corresponding to them fall outside the investigated volume of the measuring instruments, and they may even fall outside its measuring volume. This is made evident by the presence of matrix $\mathbf{E}$ in (29). This condition prevents an easy evaluation of t_{2x}, t_{2y}, and θ_2. It is then preferable to introduce the following terms $\xi_x = -\left(t_{2x} + R2\Delta\right)$, $\xi_y = -\left(t_{2y} + O2\Delta\right)$, and $\xi_\theta = -\theta_2$, which take into account part of the stage error due to non-orthogonality and scale error. For notation consistency, $\mathbf{U}_{2,x}$ and $\mathbf{U}_{2,y}$ are introduced, too:

$$\begin{aligned}
\mathbf{V}_{2,x}\mathbf{E} = \mathbf{U}_{2,x}\mathbf{E} &= \left(\left(O\mathbf{Y} + R\mathbf{X} + \mathbf{F}_x\right)\mathbf{T}_2 + \mathbf{A}_x - \theta_2\mathbf{Y} + \mathbf{1}\mathbf{1}^{\mathrm{T}}t_{2x}\right)\mathbf{E} \\
&= \left(\mathbf{F}_x\mathbf{T}_2 + O\mathbf{Y} + R\mathbf{X} + \mathbf{A}_x - \theta_2\mathbf{Y} + \left(\mathbf{1}\mathbf{1}^{\mathrm{T}}t_{2x} + R\mathbf{X}\left(\mathbf{T}_2 - \mathbf{I}\right)\right)\right)\mathbf{E} \\
&= \mathbf{F}_x\mathbf{T}_2\mathbf{E} + O\mathbf{Y}\mathbf{E} + R\mathbf{X}\mathbf{E} + \mathbf{A}_x\mathbf{E} + \xi_\theta\mathbf{Y}\mathbf{E} - \xi_x\mathbf{1}\mathbf{1}^{\mathrm{T}}\mathbf{E} \\
\mathbf{V}_{2,y}\mathbf{E} = \mathbf{U}_{2,y}\mathbf{E} &= \mathbf{F}_y\mathbf{T}_2\mathbf{E} + O\mathbf{X}\mathbf{E} - R\mathbf{Y}\mathbf{E} + \mathbf{A}_y\mathbf{E} - \xi_\theta\mathbf{X}\mathbf{E} - \xi_y\mathbf{1}\mathbf{1}^{\mathrm{T}}\mathbf{E}
\end{aligned} \tag{30}$$

Now, subtracting (16) from (30) it is possible to get rid of the scale, non orthogonality, and artifact errors:

$$\begin{aligned}
\mathbf{U}_{2,x}\mathbf{E} - \mathbf{U}_{0,x}\mathbf{E} &= \mathbf{F}_x\left(\mathbf{T}_2 - \mathbf{I}\right)\mathbf{E} + \xi_\theta\mathbf{Y}\mathbf{E} - \xi_x\mathbf{1}\mathbf{1}^{\mathrm{T}}\mathbf{E} \\
\mathbf{U}_{2,y}\mathbf{E} - \mathbf{U}_{0,y}\mathbf{E} &= \mathbf{F}_y\left(\mathbf{T}_2 - \mathbf{I}\right)\mathbf{E} - \xi_\theta\mathbf{X}\mathbf{E} - \xi_y\mathbf{1}\mathbf{1}^{\mathrm{T}}\mathbf{E}
\end{aligned} \tag{31}$$

From the first equation in Eq. (31) it is possible to evaluate ξ_x:

$$\xi_x = -\frac{\mathbf{1}^{\mathrm{T}}\left(\mathbf{U}_{2,x} - \mathbf{U}_{0,x}\right)\mathbf{E}\mathbf{E}^{\mathrm{T}}\mathbf{O}_{\mathbf{T}}^{\mathrm{T}}\mathbf{X}^{\mathrm{T}}\mathbf{1}}{\mathbf{1}^{\mathrm{T}}\mathbf{1}\mathbf{1}^{\mathrm{T}}\mathbf{E}\mathbf{E}^{\mathrm{T}}\mathbf{O}_{\mathbf{T}}^{\mathrm{T}}\mathbf{X}^{\mathrm{T}}\mathbf{1}} \tag{32}$$

where the properties that $\left(\mathbf{T}_2 - \mathbf{I}\right)\mathbf{E}\mathbf{E}^{\mathrm{T}}\mathbf{O}_{\mathbf{T}}^{\mathrm{T}}\mathbf{X}^{\mathrm{T}} = \mathbf{X}^{\mathrm{T}}$, and $\mathbf{1}^{\mathrm{T}}\mathbf{Y}$ is a row vector made up by null elements have been taken into consideration.

Determining ξ_θ is more complicated, and requires measurement results obtained in view 1. From (21) we evince that

$$\mathbf{F}_x + \mathbf{S}\mathbf{F}_x\mathbf{S} = \mathbf{P} + \mathbf{S}\mathbf{Q}^{\mathrm{T}} \tag{33}$$

which (considering that $\mathbf{S}\mathbf{T}_2 = \mathbf{T}_2^{\mathrm{T}}\mathbf{S}$) can be manipulated to obtain

$$\mathbf{F}_x\mathbf{T}_2 + \mathbf{S}\mathbf{F}_x\mathbf{T}_2^{\mathrm{T}}\mathbf{S} = \mathbf{P}\mathbf{T}_2 + \mathbf{Q}^{\mathrm{T}}\mathbf{T}_2 \tag{34}$$

The following expressions can be derived from (31) (please note the second one is obtained by pre-multiplying time $\mathbf{S}$ and post-multiplying time $\mathbf{T}_2^{\mathrm{T}}\mathbf{S}$ the first):

$$\begin{array}{llllll} \mathbf{F}_x\mathbf{T}_2 & -\mathbf{F}_x & =\mathbf{U}_{2,x} & -\mathbf{U}_{0,x} & +\xi_x\mathbf{1}\mathbf{1}^{\mathrm{T}} & -\xi_\theta\mathbf{Y} \\ \mathbf{S}\mathbf{F}_x\mathbf{S} & -\mathbf{S}\mathbf{F}_x\mathbf{T}_2^{\mathrm{T}}\mathbf{S} & =\mathbf{S}\mathbf{U}_{2,x}\mathbf{T}_2^{\mathrm{T}}\mathbf{S} & -\mathbf{S}\mathbf{U}_{0,x}\mathbf{T}_2^{\mathrm{T}}\mathbf{S} & +\xi_x\mathbf{1}\mathbf{1}^{\mathrm{T}} & -\xi_\theta\mathbf{S}\mathbf{Y}\mathbf{T}_2^{\mathrm{T}}\mathbf{S} \end{array} \tag{35}$$

By combining (33), (34), and (35) one can obtain the following expression:

$$\begin{aligned} & \left(\mathbf{F}_x\mathbf{T}_2 + \mathbf{S}\mathbf{F}_x\mathbf{T}_2^{\mathrm{T}}\mathbf{S}\right) - \left(\mathbf{F}_x + \mathbf{S}\mathbf{F}_x\mathbf{S}\right) \\ =& \mathbf{U}_{2,x} - \mathbf{U}_{0,x} - \mathbf{S}\mathbf{U}_{2,x}\mathbf{T}_2^{\mathrm{T}}\mathbf{S} + \mathbf{S}\mathbf{U}_{0,x}\mathbf{T}_2^{\mathrm{T}}\mathbf{S} - \xi_\theta\left(\mathbf{Y} - \mathbf{S}\mathbf{Y}\mathbf{T}_2^{\mathrm{T}}\mathbf{S}\right) \\ =& \mathbf{P}\mathbf{T}_2 + \mathbf{S}\mathbf{Q}^{\mathrm{T}}\mathbf{T}_2 - \left(\mathbf{P} + \mathbf{S}\mathbf{Q}^{\mathrm{T}}\right) \end{aligned} \tag{36}$$

This is a matrix equation in which the only unknown term is ξ_θ. Every element in the matrix defines an equation that can serve to evaluate ξ_θ, with the exception of those elements which correspond to null elements of $\mathbf{Y} - \mathbf{S}\mathbf{Y}\mathbf{T}_2^{\mathrm{T}}\mathbf{S}$. Please remember that the last two columns of $\mathbf{U}_{2,x}$ do not exist.

A similar result can be obtained from the $\mathbf{U}_{2,y}$ terms, starting from:

$$\begin{aligned} \mathbf{F}_y + \mathbf{S}\mathbf{F}_y\mathbf{S} &= \mathbf{Q} - \mathbf{S}\mathbf{P}^{\mathrm{T}} \\ \mathbf{F}_y\mathbf{T}_2 + \mathbf{S}\mathbf{F}_y\mathbf{T}_2\mathbf{S} &= \mathbf{Q}\mathbf{T}_2 - \mathbf{S}\mathbf{P}^{\mathrm{T}}\mathbf{T}_2^{\mathrm{T}} \end{aligned} \tag{37}$$

and obtaining:

$$\begin{aligned} & \left(\mathbf{F}_y\mathbf{T}_2 + \mathbf{S}\mathbf{F}_y\mathbf{T}_2^{\mathrm{T}}\mathbf{S}\right) + \left(\mathbf{F}_y - \mathbf{S}\mathbf{F}_y\mathbf{S}\right) \\ =& \mathbf{U}_{2,y} - \mathbf{U}_{0,y} - \mathbf{S}\mathbf{U}_{2,y}\mathbf{T}_2^{\mathrm{T}}\mathbf{S} + \mathbf{S}\mathbf{U}_{0,y}\mathbf{T}_2^{\mathrm{T}}\mathbf{S} + \xi_\theta\left(\mathbf{X} - \mathbf{S}\mathbf{X}\mathbf{T}_2^{\mathrm{T}}\mathbf{S}\right) \\ =& \mathbf{Q}\mathbf{T}_2 - \mathbf{S}\mathbf{P}^{\mathrm{T}}\mathbf{T}_2 - \left(\mathbf{Q} - \mathbf{S}\mathbf{P}^{\mathrm{T}}\right) \end{aligned} \tag{38}$$

If no random error exists, the ξ_θ solutions to every equation in (36) and (38) are equal. If some random error is present, one can take the average of the values obtained, in order to minimize the overall evaluation uncertainty.

Finally, to determine ξ_y let us consider the second expression in (31). With a procedure similar to the one adopted for the evaluation of ξ_x, the following result can be obtained:

$$\xi_y = -\frac{\mathbf{1}^{\mathrm{T}}\left(\mathbf{U}_{2,y} - \mathbf{U}_{0,y}\right)\mathbf{E}\mathbf{E}^{\mathrm{T}}\mathbf{O}_{\mathbf{T}}^{\mathrm{T}}\mathbf{X}^{\mathrm{T}}\mathbf{1} + \xi_\theta\mathbf{1}^{\mathrm{T}}\mathbf{X}\mathbf{E}\mathbf{E}^{\mathrm{T}}\mathbf{O}_{\mathbf{T}}^{\mathrm{T}}\mathbf{X}^{\mathrm{T}}\mathbf{1}}{\mathbf{1}^{\mathrm{T}}\mathbf{1}\mathbf{1}^{\mathrm{T}}\mathbf{E}\mathbf{E}^{\mathrm{T}}\mathbf{O}_{\mathbf{T}}^{\mathrm{T}}\mathbf{X}^{\mathrm{T}}\mathbf{1}} \tag{39}$$

Ye *et al.* have demonstrated similar formulas for calculating ξ_x, ξ_y, and ξ_θ when there is a translation equal to Δ in view 2. It is interesting to note that it is impossible to solve ξ_x and ξ_y for values of the shift greater than 2Δ, because a property similar to $(\mathbf{T}_2 - \mathbf{I})\,\mathbf{E}\mathbf{E}^{\mathrm{T}}\mathbf{O}_{\mathbf{T}}^{\mathrm{T}}\mathbf{X}^{\mathrm{T}} = \mathbf{X}^{\mathrm{T}}$ does not exist. In particular, it is impossible to formulate a matrix similar to $\mathbf{O}_{\mathbf{T}}$.

4.3.1. Evaluation of the central row of $\mathbf{F}_x$ *and* $\mathbf{F}_y$

It is now possible to evaluate $\mathbf{F}_x$ and $\mathbf{F}_y$ for the central row of the matrices only. Define:

$$\begin{aligned} \mathbf{F}_x\mathbf{T}_2\mathbf{E} - \mathbf{F}_x\mathbf{E} = \quad \mathbf{H}_x\mathbf{E} = \quad & \mathbf{U}_{2,x}\mathbf{E} - \mathbf{U}_{0,x}\mathbf{E} + \xi_x\mathbf{1}\mathbf{1}^{\mathrm{T}}\mathbf{E} - \xi_\theta\mathbf{Y}\mathbf{E} \\ \mathbf{F}_y\mathbf{T}_2\mathbf{E} - \mathbf{F}_y\mathbf{E} = \quad \mathbf{H}_y\mathbf{E} = \quad & \mathbf{U}_{2,y}\mathbf{E} - \mathbf{U}_{0,y}\mathbf{E} + \xi_y\mathbf{1}\mathbf{1}^{\mathrm{T}}\mathbf{E} + \xi_\theta\mathbf{X}\mathbf{E} \end{aligned} \tag{40}$$

Please note that at present the last two columns of $\mathbf{H}_x$ and $\mathbf{H}_y$ are missing. A complete knowledge of $\mathbf{H}_x$ and $\mathbf{H}_y$ would allow a complete reconstruction of $\mathbf{F}_x$ and $\mathbf{F}_y$, but is not available at present. This problem will be addressed in §4.4. However, even without these columns, based on (21) and (40) it is possible to evaluate the central element of matrices $\mathbf{F}_x$ and $\mathbf{F}_y$ and their central rows. Because this calculation does not involve full matrices, it is proposed in algebraic form.

From (21):

$$\begin{aligned} F_{x,s,s} &= \frac{1}{2}\left(P_{s,s} + Q_{s,s}\right) \\ F_{y,s,s} &= \frac{1}{2}\left(-P_{s,s} + Q_{s,s}\right) \end{aligned} \tag{41}$$

where $F_{x,h,k}$ is element belonging to h^{th} row and k^{th} column of matrix $\mathbf{F}_x$, $F_{y,h,k}$ is element (h,k) of matrix $\mathbf{F}_y$, etc.

Consider now the central row of matrices of $\mathbf{F}_x$ and $\mathbf{F}_y$, and in particular its relationship with the central rows of $\mathbf{H}_x$ and $\mathbf{H}_y$. It is easy to show that, for k even,

$$\begin{aligned} F_{x,s,N-k+1} - F_{x,s,k} &= H_{x,s,k} + H_{x,s,k+2} + \cdots + H_{x,s,N-k+1} \\ &= \sum_{i=k/2}^{(N-k+1)/2} H_{x,s,2i} \\ F_{y,s,N-k+1} - F_{y,s,k} &= H_{y,s,k} + H_{y,s,k+2} + \cdots + H_{y,s,N-k+1} \\ &= \sum_{i=k/2}^{(N-k+1)/2} H_{y,s,2i} \end{aligned} \tag{42}$$

and, for k odd,

$$\begin{aligned} F_{x,s,N-k+1} - F_{x,s,k} &= \sum_{i=(k+1)/2}^{(N-k+2)/2} H_{x,s,2i-1} \\ F_{y,s,N-k+1} - F_{y,s,k} &= \sum_{i=(k+1)/2}^{(N-k+2)/2} H_{y,s,2i-1} \end{aligned} \tag{43}$$

Combining these equation with (33) and (37) the evaluation of every term of the central row can be obtained, with the exception of element (s,s) that has already been calculated. Define then $m = k - s$. For $m > 0$, even:

$$
\begin{aligned}
F_{x,s,m} =& \frac{1}{2}\left(\sum_{i=-m/2}^{m/2-1} H_{x,s,2i+s} + P_{s,m} + Q_{m,s}\right) \\
F_{y,s,m} =& \frac{1}{2}\left(\sum_{i=-m/2}^{m/2-1} H_{y,s,2i+s} + Q_{s,m} - P_{m,s}\right) \\
F_{x,s,-m} =& \frac{1}{2}\left(-\sum_{i=-m/2}^{m/2-1} H_{x,s,2i+s} + P_{s,m} + Q_{m,s}\right) \\
F_{y,s,-m} =& \frac{1}{2}\left(-\sum_{i=-m/2}^{m/2-1} H_{y,s,2i+s} + Q_{s,m} - P_{m,s}\right)
\end{aligned}
\tag{44}
$$

A similar result can be obtained for m odd.

Unfortunately, this procedure cannot be extended to every term of $\mathbf{F}_x$ and $\mathbf{F}_y$. View 3 is then necessary. The estimate of $\mathbf{F}_x$ proposed in (44) is not good, either. In fact, every term in (44) involves a summation, and, because every term of the summation has its own uncertainty, the final uncertainty can be large. Moreover, the number of term in every summation depends on m, so the uncertainty of the single term varies and is proportional to m.

4.4. View 3

In view 3 the artifact is shifted by an amount 3Δ in the negative x direction of the measuring device reference system. As in view 0 and 1, misalignment can be expressed by the terms t_{3x}, t_{3y}, and θ_3. The measurement result can be expressed by the matrices $\mathbf{V}_{3,x}, \mathbf{V}_{3,y}$. It will be shown that it is not necessary to measure the whole plate in view 3. It is sufficient to measure the central row of the plate, and two adjacent columns (in the following, it will be supposed that columns s and $s+1$ have been measured). It is possible to express mathematically the measurement results by means of multiplication of the various matrices expressing artifact and stage error time $\mathbf{T}_{-3}$. The measurement results expression is the the following:

$$
\begin{aligned}
\mathbf{V}_{3,x} &= \mathbf{G}_x\mathbf{T}_{-3} + \mathbf{A}_x - \theta_3\mathbf{Y} + \mathbf{1}\mathbf{1}^{\mathrm{T}}t_{3x} \\
\mathbf{V}_{3,y} &= \mathbf{G}_y\mathbf{T}_{-3} + \mathbf{A}_y + \theta_3\mathbf{X} + \mathbf{1}\mathbf{1}^{\mathrm{T}}t_{3y}
\end{aligned}
\tag{45}
$$

Having obtained an evaluation of the central row of matrix $\mathbf{F}_x$ and $\mathbf{F}_y$, obtaining an evaluation of t_{3x}, t_{3y}, and θ_3 from the measurement of the central row of $\mathbf{V}_{3,x}$ and $\mathbf{V}_{3,y}$ is not hard. Please note that, having obtained O from (19) and R from (20), from (6) it is possible to evaluate the central row of $\mathbf{G}_x$ and $\mathbf{G}_y$. It is then possible to evaluate the central row of $\mathbf{A}_x$ and $\mathbf{A}_y$, too, from (10) or (13) (if a random measurement error is present, it is preferable to compute both estimates and then average them). Define then $\mathbf{v}_{3,0,x}$ the *column* vector representing the central *row* of $\mathbf{V}_{3,x}$, $\mathbf{g}_{0,x}$ is the central *row* of $\mathbf{G}_x$, etc. The evaluation of t_{3x} follows simply by

$$t_{3x} = \frac{\mathbf{1}^{\mathrm{T}}{}_{N-3}\mathbf{E}_3^{\mathrm{T}}\mathbf{T}^{\mathrm{T}}{}_3\mathbf{v}_{3,0,x} - \mathbf{1}^{\mathrm{T}}{}_{N-3}\mathbf{E}_3^{\mathrm{T}}\mathbf{T}^{\mathrm{T}}{}_3\mathbf{g}_{0,x}\mathbf{T}_{-3} - \mathbf{1}^{\mathrm{T}}{}_{N-3}\mathbf{a}_{0,x}}{\mathbf{1}^{\mathrm{T}}_{N-3}\mathbf{E}_3^{\mathrm{T}}\mathbf{T}^{\mathrm{T}}{}_3\mathbf{1}} \tag{46}$$

Considering now measurement results in direction y, it is possible to write

$$\mathbf{E}_3^{\mathrm{T}}\mathbf{T}^{\mathrm{T}}{}_3\mathbf{v}_{3,0,y} - \mathbf{E}_3^{\mathrm{T}}\mathbf{T}^{\mathrm{T}}{}_3\mathbf{g}_{0,y}\mathbf{T}_{-3} - \mathbf{E}_3^{\mathrm{T}}\mathbf{T}^{\mathrm{T}}{}_3\mathbf{a}_{0,y} = \theta_3\mathbf{x} + t_{3y}\mathbf{E}_3^{\mathrm{T}}\mathbf{T}^{\mathrm{T}}{}_3\mathbf{1} \tag{47}$$

This is a matrix equation which can be solved through the least squares.

4.4.1. Obtaining the missing parts of the Fourier transforms of $\mathbf{F}_x$ and $\mathbf{F}_y$

Misalignment, scale, and non orthogonality parameters for every view have been evaluated. It is then possible to get rid of misalignment, scale, and non orthogonality errors. This is done by introducing the $\mathbf{C}$ matrices:

$$\begin{aligned}
\mathbf{C}_{0,x} &= \mathbf{U}_{0,x} - O\mathbf{Y} - R\mathbf{X} && = \mathbf{F}_x + \mathbf{A}_x \\
\mathbf{C}_{0,y} &= \mathbf{U}_{0,y} - O\mathbf{X} + R\mathbf{Y} && = \mathbf{F}_y + \mathbf{A}_y \\
\mathbf{C}_{2,x} &= \mathbf{U}_{2,x} - O\mathbf{Y} - R\mathbf{X} - \xi_\theta\mathbf{Y} + \xi_x\mathbf{1}\mathbf{1}^{\mathrm{T}} && = \mathbf{F}_x\mathbf{T}_2 + \mathbf{A}_x \\
\mathbf{C}_{2,y} &= \mathbf{U}_{2,y} - O\mathbf{X} + R\mathbf{Y} + \xi_\theta\mathbf{X} + \xi_y\mathbf{1}\mathbf{1}^{\mathrm{T}} && = \mathbf{F}_y\mathbf{T}_2 + \mathbf{A}_y \\
\mathbf{C}_{3,x} &= \mathbf{V}_{3,x} + (-O\mathbf{Y} - R\mathbf{X})\,\mathbf{T}_{-3} + \theta_3\mathbf{Y} - t_{3x}\mathbf{1}\mathbf{1}^{\mathrm{T}} && = \mathbf{F}_x\mathbf{T}_{-3} + \mathbf{A}_x \\
\mathbf{C}_{3,y} &= \mathbf{V}_{3,y} + (-O\mathbf{X} + R\mathbf{Y})\,\mathbf{T}_{-3} - \theta_3\mathbf{X} - t_{3y}\mathbf{1}\mathbf{1}^{\mathrm{T}} && = \mathbf{F}_y\mathbf{T}_{-3} + \mathbf{A}_y
\end{aligned} \tag{48}$$

As (48) shows, $\mathbf{C}$ matrices are different linear combination of the $\mathbf{F}_x, \mathbf{F}_y, \mathbf{A}_x, \mathbf{A}_y$ matrices. It is also apparent that it is possible to get rid of the $\mathbf{A}_x, \mathbf{A}_y$ terms by adding up or subtracting the various $\mathbf{C}$ matrices. Unfortunately, only the $\mathbf{C}_{0,x}$ and $\mathbf{C}_{0,y}$ matrices are actually complete - the others lack some columns, in particular those deriving from view 2 lack the last two columns, and those deriving from view 3 lack the first three columns. It is therefore necessary to "build" the missing columns. Express $\mathbf{H}_x, \mathbf{H}_y$ as a function of $\mathbf{C}_{0,x}, \mathbf{C}_{0,y}, \mathbf{C}_{2,x}, \mathbf{C}_{2,y}$, pointing out the absence of the last two columns:

$$\begin{aligned}
\mathbf{H}_x\mathbf{E} = \mathbf{F}_x\mathbf{T}_2\mathbf{E} - \mathbf{F}_x\mathbf{E} &= \mathbf{C}_{2,x}\mathbf{E} - \mathbf{C}_{0,x}\mathbf{E} \\
\mathbf{H}_y\mathbf{E} = \mathbf{F}_y\mathbf{T}_2\mathbf{E} - \mathbf{F}_y\mathbf{E} &= \mathbf{C}_{2,y}\mathbf{E} - \mathbf{C}_{0,y}\mathbf{E}
\end{aligned} \tag{49}$$

Please note that every element of $\mathbf{H}_x, \mathbf{H}_y$ could be written as

$$\begin{aligned}
H_{x,h,k} &= F_{x,h,k+2} - F_{x,h,k} \\
H_{y,h,k} &= F_{y,h,k+2} - F_{y,h,k}
\end{aligned} \tag{50}$$

It is then apparent that the knowledge of the last two columns of $\mathbf{H}_x, \mathbf{H}_y$ would require the knowledge of $F_{x,h,N+1}, F_{x,h,N+2}, F_{y,h,N+1}, F_{y,h,N+2}$. These terms have no physical meaning, in fact they may even fall outside the measuring volume of the measuring instrument. However, it is possible to solve the last two columns by supposing, without loss of generality, that $\mathbf{F}_x$ and $\mathbf{F}_y$ are *periodical* outside the inspected volume. This condition translates into the following statements:

$$\begin{aligned} F_{x,N+1,n} &= F_{x,1,n} \\ F_{y,N+1,n} &= F_{y,1,n} \\ F_{x,N+2,n} &= F_{x,2,n} \\ F_{y,N+2,n} &= F_{y,2,n} \end{aligned} \tag{51}$$

With these assumptions it is now possible to define the last two columns of $\mathbf{H}_x$ and $\mathbf{H}_y$; suppose that $(N-1)/2$ is even (the solution in case $(N-1)/2$ is odd is similar):

$$\begin{aligned} H_{x,h,N-1} =& F_{x,h,N+1} - F_{x,h,N-1} \\ =& F_{x,h,1} - F_{x,h,N-1} \\ =& -\left\{F_{x,h,N-1} - F_{x,h,1}\right\} \\ =& -\left\{\begin{array}{l} \quad F_{x,h,N-1} - F_{x,h,N-3} + F_{x,h,N-3} - F_{x,h,N-5} + \cdots + \\ +F_{x,h,s+3} - F_{x,h,s+1} + F_{x,h,s+1} - F_{x,h,s-2} + F_{x,h,s-2} - F_{x,h,s-4} + \cdots + \\ +F_{x,h,5} - F_{x,h,3} + F_{x,h,3} - F_{x,h,1} \end{array}\right\} \\ =& -\sum_{m=(s+1)/2}^{s} \left(C_{2,x,h,2m} - C_{0,x,h,2m}\right) - \sum_{m=0}^{(s-5)/2} \left(C_{2,x,h,2m+1} - C_{0,x,h,2m+1}\right) \\ & - C_{0,x,h,s+1} + C_{3,x,h,s+1} \end{aligned} \tag{52}$$

$$\begin{aligned} H_{x,h,N} =& F_{x,h,N+2} - F_{x,h,N} \\ =& F_{x,h,2} - F_{x,h,N} \\ =& -\left\{F_{x,h,N} - F_{x,h,2}\right\} \\ =& -\left\{\begin{array}{l} \quad F_{x,h,N} - F_{x,h,N-2} + F_{x,h,N-2} - F_{x,h,N-4} + \cdots + \\ +F_{x,h,s+2} - F_{x,h,s} + F_{x,h,s} - F_{x,h,s-3} + F_{x,h,s-3} - F_{x,h,s-5} + \cdots + \\ +F_{x,h,6} - F_{x,h,4} + F_{x,h,4} - F_{x,h,2} \end{array}\right\} \\ =& -\sum_{m=(s-1)/2}^{s} \left(C_{2,x,h,2m+1} - C_{0,x,h,2m+1}\right) - \sum_{m=1}^{(s-5)/2} \left(C_{2,x,h,2m} - C_{0,x,h,2m}\right) \\ & - C_{0,x,h,s} + C_{3,x,h,s} \end{aligned} \tag{53}$$

Similar expressions may be proposed also for $\mathbf{H}_y$.

Now, let us take the Fourier transform of $\mathbf{H}_x$ and $\mathbf{H}_y$:

$$\begin{aligned} \mathbf{W}\mathbf{H}_x\mathbf{W} = \mathbf{W}\mathbf{F}_x\mathbf{T}_2\mathbf{W} - \mathbf{W}\mathbf{F}_x\mathbf{W} &= \mathbf{W}\mathbf{F}_x\mathbf{W}\left(N\mathbf{W}\mathbf{S}\mathbf{T}_2\mathbf{W} - \mathbf{I}\right) \\ \mathbf{W}\mathbf{H}_y\mathbf{W} = \mathbf{W}\mathbf{F}_y\mathbf{T}_2\mathbf{W} - \mathbf{W}\mathbf{F}_y\mathbf{W} &= \mathbf{W}\mathbf{F}_y\mathbf{W}\left(N\mathbf{W}\mathbf{S}\mathbf{T}_2\mathbf{W} - \mathbf{I}\right) \end{aligned} \tag{54}$$

$N\mathbf{WST}_2\mathbf{W}-\mathbf{I}$ is a diagonal matrix. Unfortunately, its (s,s) element is equal to 0, so $N\mathbf{WST}_2\mathbf{W}-\mathbf{I}$ cannot be inverted. Define then $\mathbf{Z}$ as a diagonal matrix whose elements are the inverse of the diagonal elements of $N\mathbf{WST}_2\mathbf{W}-\mathbf{I}$, with the exception of the (s,s) element, whose value is not relevant. (54) can be rewritten as

$$\begin{aligned} \mathbf{WF}_x\mathbf{W} &\simeq \mathbf{WH}_x\mathbf{WZ} \\ \mathbf{WF}_y\mathbf{W} &\simeq \mathbf{WH}_y\mathbf{WZ} \end{aligned} \tag{55}$$

In (55) the symbol $\simeq$ remembers that the equality does not comprehend the central column of the matrices. However, remember that the real part of $\mathbf{WF}_x\mathbf{W}$ and $\mathbf{WF}_y\mathbf{W}$ is already known by (27): because the imaginary part of the central *rows* is known, (28) can be used to determine the imaginary part of the central *columns*. Finally, (7) constrains the central element of $\mathbf{WF}_x\mathbf{W}$ and $\mathbf{WF}_y\mathbf{W}$ to be equal to 0.

The knowledge of the transforms of $\mathbf{F}_x$ and $\mathbf{F}_y$ is of course equivalent to the knowledge of $\mathbf{F}_x$ and $\mathbf{F}_y$, thus solving the self-calibration problem. Anyway, to minimize uncertainty Ye *et al.*suggest to use results obtained from view 2 (and in our case from view 3, too) as little as possible. This because measurements obtained in view 2 and 3 tend to more affected by the presence of noise, which is due to the complex evaluation of their misalignment parameters. Moreover, the diagonal elements of matrix $\mathbf{Z}$ act as uncertainty amplification factors. Therefore it is suggested to calculate the real part of the transform by means of (27), and to calculate the imaginary part using those cells of $\mathbf{WH}_x\mathbf{WZ}$ and $\mathbf{WH}_y\mathbf{WZ}$ which correspond to the lower values of the diagonal elements of $\mathbf{Z}$, that is, either directly applying (55) when the corresponding diagonal element is low, or applying (28) when the corresponding diagonal element is high.

5. Algorithm test

The algorithm has been tested by means of simulation.

A plate has been simulated. The plate has $N = 25$ and $\Delta = 1$ mm. Fig. 2 shows the artifact errors. Practically speaking, this image shows matrices $\mathbf{A}_x$ and $\mathbf{A}_y$. Each arrow represents the location error of a sub-artifact with respect to its nominal position. Artifact errors have been generated according to a non correlated Gaussian distribution, with null expected value and 0.001 mm standard deviation.

Based on this grid, the corresponding error map $\mathbf{G}_x$ and $\mathbf{G}_y$ has been simulated, as shown in Fig. 3. The error map has been generated considering the following parameters: the non-orthogonality error O and the scale error R are both equal to 0.00001. Both the second order error terms $\mathbf{F}_x$ and $\mathbf{F}_y$ have been generated according to a Spatially correlated Autoregressive model of the first order (SAR(1)) [21]. A SAR(1) model is a statistic model in which the data are not uncorrelated, but share a *spatial* correlation, so elements which are close to each other tend to show similar values. In formula, for, e.g., $\mathbf{F}_x$,

$$F_{x,h,k} = \rho_x \sum_{i,j} w_{i,j}^{h,k} F_{x,i,j} + \varepsilon_{x,h,k} \tag{56}$$

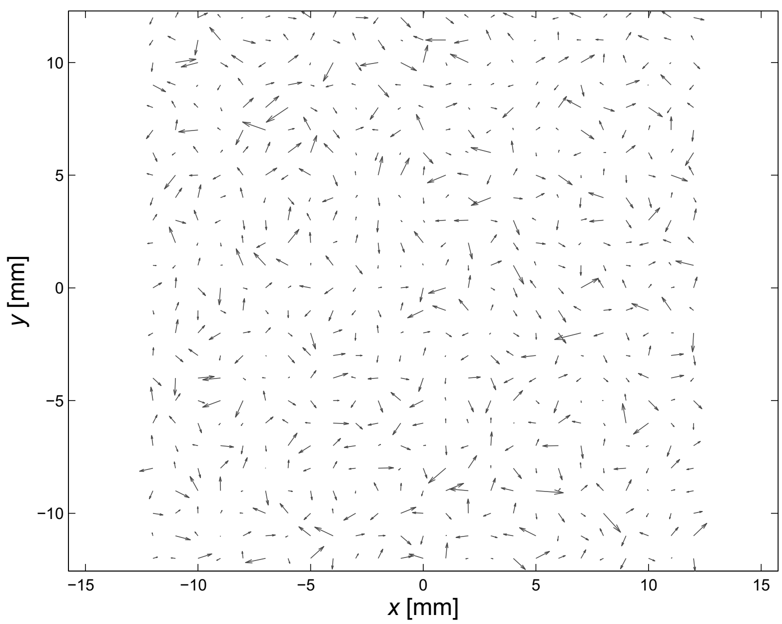

Figure 2: Artifact error - representation of $\mathbf{A}_x$ and $\mathbf{A}_y$ matrices.

where $\varepsilon_{x,h,k}$ is a white noise, ρ_x is a correlation coefficient (larger values of ρ denote a stronger correlation) and $w_{i,j}^{h,k}$ represents the generic element of the *adjacency matrix* (or *spatial weights matrix*) for the first order neighborhood. In other words, $w_{i,j}^{h,k}$ is set equal to 1 if the (i, j) point is the neighbor of the (h, k) point and 0 otherwise (see [21] for further details). In the present simulation $\rho_y = \rho_x = 0.9$, and the standard deviation of $\varepsilon_{x,h,k}$ and $\varepsilon_{y,h,k}$ varies, in order to investigate its impact on the method accuracy. This way, the total simulated dispersion σ_G of $\mathbf{G}_x$ and $\mathbf{G}_y$ is in the range 0.1 - 10 µm.

Error map and artifact error have then been combined to simulate views according to (10), (13), (29), and (45). In every simulation a random misalignment error has been added, that is, misalignment parameters $t_{\alpha x}$, $t_{\alpha y}$ and θ_α have been simulated according a Gaussian statistical distribution with null expected value and standard deviation equal to 0.0001 mm for $t_{\alpha x}$, $t_{\alpha y}$ and 0.0001 rad for θ_α.

If no random measurement error is present, the algorithm is able to evaluate the exact value of every parameter or error described so far. In order to evaluate the impact of the measurement error on the accuracy of the evaluated error map, a simulation has been conducted.

Finally, a random measurement noise has been added to the simulated measurements. The noise has been simulated according a gaussian distribution with

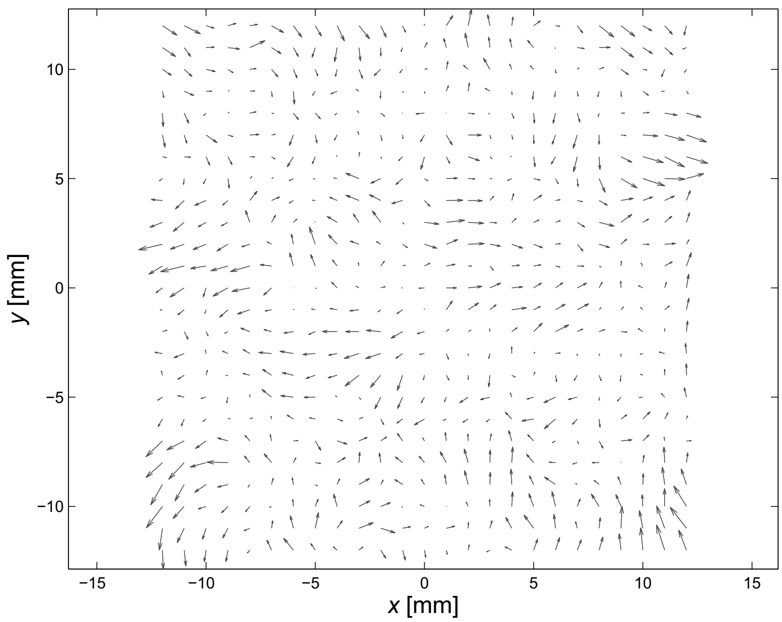

Figure 3: Error map - representation of $\mathbf{G}_x$ and $\mathbf{G}_y$ matrices.

zero mean and standard deviation σ_r in the range 0.001 - 10 µm.

Simulation results are reported in terms of standard deviation (the average error has been found to be null on average). In practice, $\hat{\mathbf{G}}_x - \mathbf{G}_x$ and $\hat{\mathbf{G}}_y - \mathbf{G}_y$ are calculated, where $\hat{\mathbf{G}}_x$ and $\hat{\mathbf{G}}_y$ represent the estimated error map, and then the sample standard deviation σ_C of all the values contained in $\hat{\mathbf{G}}_x - \mathbf{G}_x$ and $\hat{\mathbf{G}}_y - \mathbf{G}_y$ is calculated. Fig. 4 proposes results for the standard deviation, plotting σ_C as a function of standard deviation of the measurement noise σ_r and the total dispersion of the stage error σ_G. The plot shows that σ_C does not depend on σ_G: the method is able to estimate the stage error even when it is large. σ_C is about the same order of magnitude of σ_r. In general, as the stage error estimate adds up errors from several sub-artifact measurement, the estimate standard deviation tends to be slightly larger than the random noise standard deviation. This magnification effect on the standard deviation deserves a deeper study. Fig. 5 plots the standard deviation of the estimate error σ_C as a function of σ_r and the number of rows and columns of sub-artifacts N. It is evident that the dependence of σ_C on N is approximately linear regardless of the value σ_r. This effect had already been highlighted by Ye *et al.*when he translation is equal to Δ. The magnitude of the increase of σ_C due to an increase of N is similar in Ye *et al.*'s method and the proposed method.

A way of improving precision of the estimate of $\mathbf{G}_x$ and $\mathbf{G}_y$ is of course by

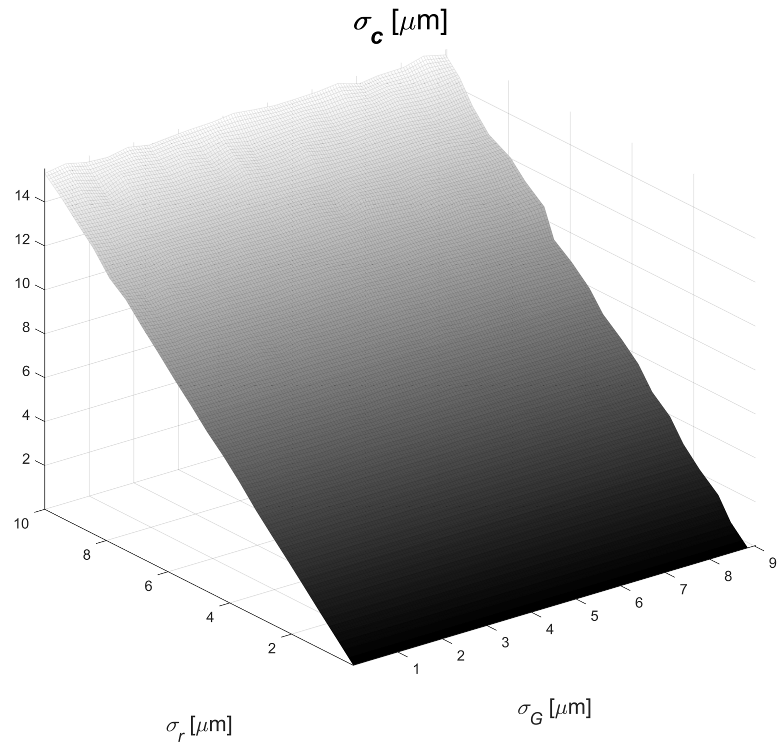

Figure 4: Standard deviation of the estimate error σ_C as a function of σ_r and σ_G.

repeating the measurement and averaging the results. Moreover, in coordinate measuring systems most of the times each sub-artifact is not measured on a single sampling point, but on many sampling points that are then fitted. As, such the random noise for the single sub-artifact measurement is usually lower than the measuring system probing error.

6. Conclusions and final remarks

A methodology for self-calibrating 2D linear stages has been proposed. This methodology involves the measurement of an uncalibrated artifact in four different views. Every sub-artifact that can be sampled has to be sampled in every view, with the exception of the last view, in which only two columns and a row have to be measured. If the experimental effort of the original methodology proposed by Ye *et al.* is compared to the effort required by this methodology, one can point out that they differ for $2N-2$ measurements of sub-artifacts, so the experimental effort is not much larger. This methodology should allow the self-calibration when a shift equal to Δ is too small to be easily obtained.

It is also worth noting that the methodology results also in the calibration

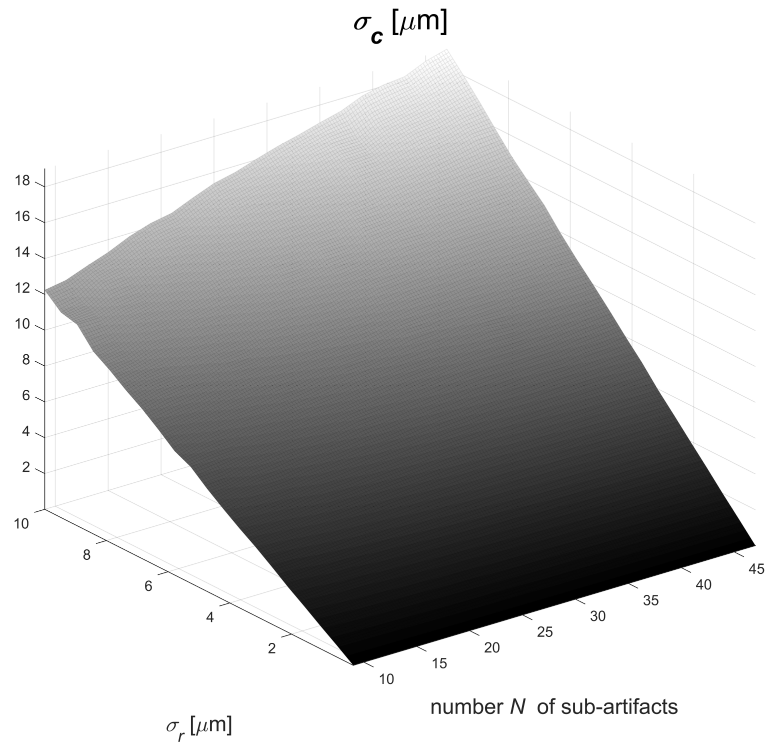

Figure 5: Standard deviation of the estimate error σ_C as a function of σ_r and the number of rows and columns of sub-artifacts N.

of the plate used for the tests. As such, the self calibration can be tested by adding a view taken with the plate e.g. 180° rotated.

Although this paper does not compare the proposed method to any method other than Ye *et al.*'s, its performance is absolutely comparable to those of the latter. The comparison of Ye *et al.*'s method to other methods can be found in the papers reported in the bibliography.

Self-calibration methodologies are useful when calibrated artifacts would be too expensive to be manufactured and maintained. In fact, the artifact adopted can be uncalibrated and not even particularly accurate. However, the main limitation of self-calibration methodologies is that they cannot guarantee metrological traceability. In the proposed methodology, the no-magnification hypothesis expresses this limit: traceability is required a priori. How to solve this limitation (with a limited increase in experimental activity) will be investigated.

Bibliography

[1] ISO/IEC, ISO/IEC GUIDE 99:2007(E/F): International vocabulary of metrology - basic and general concepts and associated terms (VIM) (2007).

[2] P. Pedone, E. Audrito, A. Balsamo, Compensation of CMM geometrical errors by the GEMIL technique: Experimental results, CIRP Annals - Manufacturing Technology 63 (1) (2014) 489–492.

[3] C. J. Evans, R. J. Hocken, W. T. Estler, Self-calibration: Reversal, redundancy, error separation, and 'absolute testing', CIRP Ann - Manuf Technol 45 (2) (1996) 617–634.

[4] R. J. Hocken, "reversal" techniques for coordinate measuring machine calibration, in: R. J. Hocken, P. H. Pereira (Eds.), Coordinate Measuring Machines and Systems, 2nd Edition, CRC Press, Boca Raton, New York, 2012, Ch. 13, pp. 361–370.

[5] S. Sartori, G. X. Zhang, Geometric error measurement and compensation of machines, CIRP Ann - Manuf Technol 44 (2) (1995) 599–609.

[6] H. Schwenke, W. Knapp, H. Haitjema, A. Weckenmann, R. Schmitt, F. Delbressine, Geometric error measurement and compensation of machines - an update, CIRP Ann - Manuf Technol 57 (2) (2008) 660 – 675.

[7] J. Ye, M. Takac, C. N. Berglund, G. Owen, R. F. Pease, An exact algorithm for self-calibration of two-dimensional precision metrology stages, Precis. Eng. 20 (1) (1997) 16–32.

[8] S. Yoo, S.-W. Kim, Self-calibration algorithm for testing out-of-plane errors of two-dimensional profiling stages, Int. J. Mach. Tools Manuf 44 (7-8) (2004) 767–774.

[9] Q. Dang, S. Yoo, S.-W. Kim, Complete 3-D Self-calibration of Coordinate Measuring Machines, CIRP Ann - Manuf Technol 55 (1) (2006) 527–530.

[10] C. Hu, Y. Zhu, J. Hu, M. Zhang, D. Xu, A holistic self-calibration algorithm for xy precision metrology systems, IEEE Trans. Instrum. Meas. 61 (9) (2012) 2492–2500.

[11] Y. Zhu, C. Hu, J. Hu, M. Zhang, D. Xu, On-axis self-calibration of precision XYθz metrology systems: An approach framework, in: Proceedings of the 2013 IEEE/ASME International Conference on Advanced Intelligent Mechatronics: Mechatronics for Human Wellbeing, 2013, pp. 1078–1083.

[12] Y. Zhu, C. Hu, J. Hu, K. Yang, Accuracy-and simplicity-oriented self-calibration approach for two-dimensional precision stages, IEEE Trans. Ind. Electron. 60 (6) (2013) 2264–2272.

[13] C. Hu, Y. Zhu, J. Hu, D. Xu, M. Zhang, A holistic self-calibration approach for determination of three-dimensional stage error, IEEE Trans. Instrum. Meas. 62 (2) (2013) 483–494.

[14] C. Hu, Y. Zhu, J. Hu, D. Xu, M. Zhang, An on-axis self-calibration approach for precision rotary metrology stages based on an angular artifact plate, Meas. Sci. Technol. 24 (8) (2013) 085007.

[15] P. Ekberg, L. Stiblert, L. Mattsson, A new general approach for solving the self-calibration problem on large area 2d ultra-precision coordinate measurement machines, Meas. Sci. Technol. 25 (5) (2014) 055001.

[16] P. Ekberg, L. Stiblert, L. Mattsson, Z-correction, a method for achieving ultraprecise self-calibration on large area coordinate measurement machines for photomasks, Meas. Sci. Technol. 25 (5) (2014) 055002.

[17] D. Wang, X. Chen, Y. Xu, T. Guo, M. Kong, J. Zhao, B. Zhang, B. Zhu, Stage error calibration for coordinates measuring machines based on self-calibration algorithm, Precis. Eng. 41 (2015) 86–95.

[18] T. D. Lemmons, R. J. Hocken, J. L. Overcash, Macroscopic transfer artifact for nano-positioning, in: Proceedings of the 26th Annual Meeting of the American Society for Precision Engineering, Vol. 52, 2011, pp. 315–318.

[19] S. Petrò, Support script for the article "a double shift self-calibration method for micro xy stages", Published on Mendeley (2018). URL `http://dx.doi.org/10.17632/544c8pmzw5.2`

[20] R. N. Bracewell, The Fourier Transform and it's Applications, McGraw-Hill, 2000.

[21] N. A. C. Cressie, Statistics for Spatial Data, 1st Edition, Wiley-Interscience, New York, 1993.